Emission characteristics of water in the Universe

Poelman, Dieter Roel

Chapter 1

Introduction and outline

1.1 The interstellar medium

The splendor of a night sky filled with glowing stars is one of the truly remarkable experiences of life. At first glance, the space between the stars seems to be empty, however, there must be some material from which stars can form. As we look more carefully at the interstellar space, we find that it is filled with a diffuse gas laced with microscopic dust particles. This combination of gas and dust is called the *interstellar medium* (ISM) and is the raw material from which stars are being formed. This material is found throughout the Universe, though mainly concentrated within galaxies, with very little found in between galaxies. The amount of ISM in the Milky Way is $\sim 10\%$ of the stellar content by mass, the latter being $10^{11}\,M_\odot$. While dense regions are interweaved throughout the ISM, the overall density is extremely low, lower than that of the best vacuum routinely created in laboratories on Earth. However, the low density is compensated by the amount of matter adding up over the vast distances between the stars.

Interstellar gas consists mostly of neutral atoms, e.g., hydrogen (H) and helium (He), molecules, e.g., H_2, CO, H_2O, as well as charged particles such as ions and electrons. Beyond the large amounts of H, some He, and small amounts of lithium (Li) created during the Big Bang, other elements that constitute stars and their planets were produced via nucleosynthesis in the interiors of stars or through supernova (SN) explosions of high-mass stars. As a result, the elements out of which our own solar system is formed are a mix of nucleosynthetic products from many generations of stars. This molecular evolution connects a variety of processes that create more complex molecules or destroy them. Molecular complexity in the ISM is driven particularly in molecular clouds, as star formation exclusively takes place in these regions. Up to now, around 130 different molecules have been iden-

tified in the ISM and more are still waiting to be discovered. On the other hand, dust is formed in circumstellar envelopes of late-type stars where the physical conditions are favourable for complex silicates and carbonaceous material to grow. The chemistry of the dust depends on the C/O ratio. As the CO molecule is very tightly bound, it consumes all available C or O, whichever is less abundant. If C is left over after the formation of CO, then a C-based dust chemistry occurs. Conversely, silicate dust forms in an O-rich environment.

Astrochemistry, the study of the chemical interactions between the gas and dust in space, is complex because of the enormous range of environments present therein, each with its specific density and temperature range. Among interstellar components are (i) the Hot Ionized Medium (HIM, $T \sim 10^6$ K, $n_{\rm H} \sim 3 \times 10^{-3}$ cm^{-3}), (ii) the Warm Ionized Medium (WIM, $T \sim 10^4$ K, $n_{\rm H} > 10$ cm^{-3}), (iii) the Warm Neutral Medium (WNM, $T \sim 10^{3-4}$ K, $n_{\rm H} \sim 0.1$ cm^{-3}), (iv) the atomic Cold Neutral Medium (CNM, $T \sim 100$ K, $n_{\rm H} \sim 10-100$ cm^{-3}), (v) the molecular Cold Neutral Medium (CNM, $T \sim 10-50$ K, $n_{\rm H_2} \sim 10^{3-5}$ cm^{-3}), and (vi) molecular hot cores ($T \sim 100-300$ K, $n_{\rm H_2} > 10^6$ cm^{-3}). Throughout these regions, each chemical species is associated with a unique spectrum. Not only do atoms have characteristic spectra, so do molecules as well. These objects emit and absorb electromagnetic radiation at certain definite frequencies, which range from the radio frequency region up to the region of very short wavelength X-rays, or gamma rays. Moreover, each chemical element produces its own characteristic emission and absorption line spectra, depending on the temperature and density distributions of the gas and dust in previously mentioned regions. Hence, it is through the interpretation of the observed emission or absorption of radiation at characteristic frequencies coming from atoms and molecules that we learn more about astronomical objects. As such, the interplay between gas, dust and radiation enables us to retrieve information from various sites in the Universe.

As the water molecule is the cornerstone of this thesis, in the following, we will highlight some important aspects related to the formation and destruction processes (Section 1.2), its spectral properties (Section 1.3), and the observational signatures (Section 1.4) of the molecule.

1.2 Formation and destruction routes of H_2O

Behind the apparent simplicity of the water molecule lies a rich chemistry at the origin, since water can be formed via various routes in the solid-phase, i.e., on dust grains, as well as through gas-phase reactions. Because of this variety, in the following focus is on the most important formation and destruction pathways.

(i) In cold gas ($T < 100$ K), the temperatures are too low for endoergic reactions to take place. Therefore, in this regime, H_2O is formed mainly through the dissociative recombination of the H_3O^+ ion:

$$H_3O^+ + e^- \rightarrow H_2O + H \qquad (+6.4\,\mathrm{eV}). \tag{1.1}$$

Note that at these low temperatures H_3O^+ itself is produced in a reaction sequence of H_3^+ with O to form OH^+, followed by molecular hydrogen (H_2) reactions leading to H_3O^+, and no H_2O is needed a priori. The H_3^+ formation rate in its turn is proportional to the ionization rate of H_2 (and He) due to cosmic- and/or X-rays. It is found that quiescent low-temperature ($T \lesssim 230$ K) gas-phase chemistry accounts for typical H_2O abundances of up to a few times 10^{-7} (e.g., Lee et al. 1996; Le Teuff et al. 2000).

In addition, at these low temperatures, H_2O can be formed on interstellar grain surfaces via hydrogenation of surface oxygen atoms by hydrogen atoms which land on the grain, owing to the high mobility of atomic hydrogen on the cold surfaces. When temperatures reach ~ 100 K, i.e., the sublimation temperature of H_2O, water evaporates from dust grains into the gas-phase. Conversely, at temperatures lower than the sublimation temperature water is frozen-out onto dust grains and thus removed from the gas-phase. Note that the freeze-out of water onto grain surfaces is a function of density and time, i.e., high densities and timescales $t > 10^6$ yr favour the depletion of species (Bergin 1995). Besides this, in cold dark clouds, water ice can be destroyed through photodesorption via external or internal ultraviolet and infrared photons (Adamson et al. 1988; Williams, Hartquist & Whittet 1992; Smith et al. 1993).

(ii) At temperatures above a few 100 K, e.g., in hot core regions and shocked gas, H_2O will be produced rapidly from O by a series of two neutral-neutral reactions whose activation barriers are overcome by the thermal energy of the warm gas. First, a substantial fraction of the oxygen will be transformed into OH initiated by the endothermic reaction

$$O + H_2 \rightarrow OH + H \qquad (-0.5\,\mathrm{eV}), \tag{1.2}$$

subsequently followed by

$$OH + H_2 \rightarrow H_2O + H, \tag{1.3}$$

a reaction which possesses a large activation barrier. Quiescent gas-phase chemistry predicts H_2O abundances of up to $\sim 10^{-4}$ for $T \gtrsim 230$ K by these reactions (Charnley 1997; Doty et al. 2002). Note, however, that these high water abundances at high T require a high H_2/H ratio to prevent back reactions with atomic H.

(iii) Water is not only formed through an oxygen-rich chemistry as previously mentioned, but also in a carbon-rich environment, e.g., a circumstellar envelope around a carbon-rich asymptotic giant branch (AGB) star, or in inner regions of protoplanetary disks, by a process called Fischer-Tropsch catalysis. This process is defined as the reaction whereby CO and H_2 are converted into hydrocarbons on an iron or nickel catalyst and water is produced as a by-product. The process can be summarized by

$$CO + 3H_2 \rightarrow CH_4 + H_2O. \tag{1.4}$$

In the gas-phase, this type of reaction has a high activation energy that prevents its occurrence. However, the presence of a transition metal catalyst dramatically lowers the barrier to reaction. It has been shown that these kinds of reactions can produce sufficient gaseous water to account for the observations in carbon-rich environments (Willacy 2004). The amount of water produced in this way obviously depend on the abundance of the catalyst metal grains.

(iv) Photodissociation of water occurs in the vicinity of a strong ultraviolet (UV, $6-13.6\,\mathrm{eV}$) radiation field, e.g., impinging radiation of a nearby star on a molecular cloud, where

$$H_2O + h\nu \rightarrow H + OH, \tag{1.5}$$

and

$$OH + h\nu \rightarrow O + H. \tag{1.6}$$

Note that the dissociation of OH into O and H already prevents the formation of H_2O.

(v) Finally, water destruction by X-rays becomes important in the proximity of an X-ray source, e.g., in envelopes around young stellar objects (YSOs). X-rays can reduce the water abundance from their 10^{-4} peak in these regions, especially where the gas temperature drops below 230 K for X-ray fluxes $F_X \gtrsim 10^{-5}$–$10^{-4}\,\mathrm{erg\,cm^{-2}\,s^{-1}}$ (Stäuber et al. 2006). The converse is also true. Meijerink & Spaans (2005) have shown that the abundance of water can be enhanced in the vicinity of an X-ray source, like an accreting black hole, where for $n_H \sim 10^5\,\mathrm{cm^{-3}}$ and $F_X \gtrsim 1\,\mathrm{erg\,cm^{-2}\,s^{-1}}$ abundances of $\sim 10^{-5}$–10^{-6} are found for $T \sim 500$ K. Note that the latter is mainly a temperature effect (see Eq. 1.2 and 1.3). However, X-rays also maintain a larger ionization fraction and promote charge transfer between H^+ and O. As a result, the reaction chain $O^+ + H_2 \rightarrow OH^+$, $OH^+ + H_2 \rightarrow H_2O^+$, $H_2O^+ + H_2 \rightarrow H_3O^+$ leads to the formation of H_3O^+, and is followed by the dissociative recombination of H_3O^+ to O, OH, and H_2O.

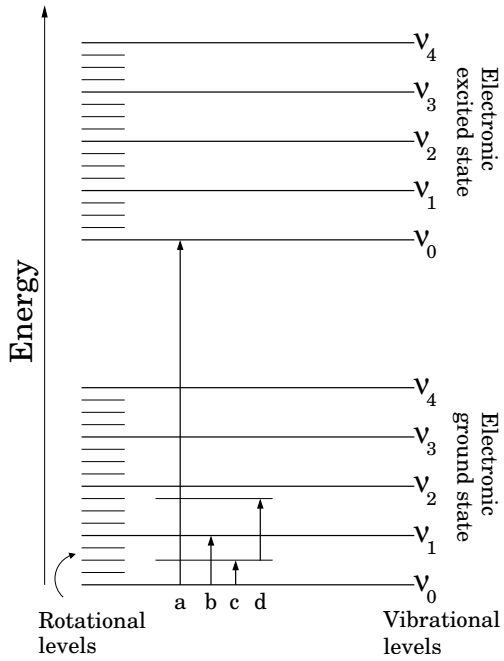

Figure 1.1: Molecular energy level diagram. (a) Electronic, (b) vibrational and (c) rotational transitions, as well as (d) ro-vibrational transitions are displayed.

1.3 Structure of the water molecule – spectroscopy

Spectroscopy, the study of the interaction of electromagnetic radiation (visible light, radio waves, X-rays, etc.) with matter, is the key to reveal the behaviour of the molecule through an observed spectrum. Spectra of the same molecule change as the molecule reacts in a different manner on various types of energy sources. Visible and UV light are energetic enough to promote the redistribution of electrons in a molecule such that the electronic potential energy of the molecule is changed, i.e., electrons will occupy a different set of energy levels. This redistribution of the electrons leads to the excitation, de-excitation, and/or ionization of the molecule. Hence, we call visible and UV spectroscopy *electronic spectroscopy*. Light of infrared frequencies can generally promote molecules from one vibrational energy level to another. Therefore, a synonym of infrared spectroscopy is *vibrational spectroscopy*. Note that light of energy sufficient to cause electronic transitions ($E \gtrsim 5000\,\mathrm{K}$) usually – depending on selection rules – simultaneously promotes vibrational ($100\,\mathrm{K} \lesssim E \lesssim 1000\,\mathrm{K}$) and rotational transitions ($E \sim 10\,\mathrm{K}$), as vibrational and rotational energies of molecules are even smaller than electronic energies. By the 'excitation' of electrons,

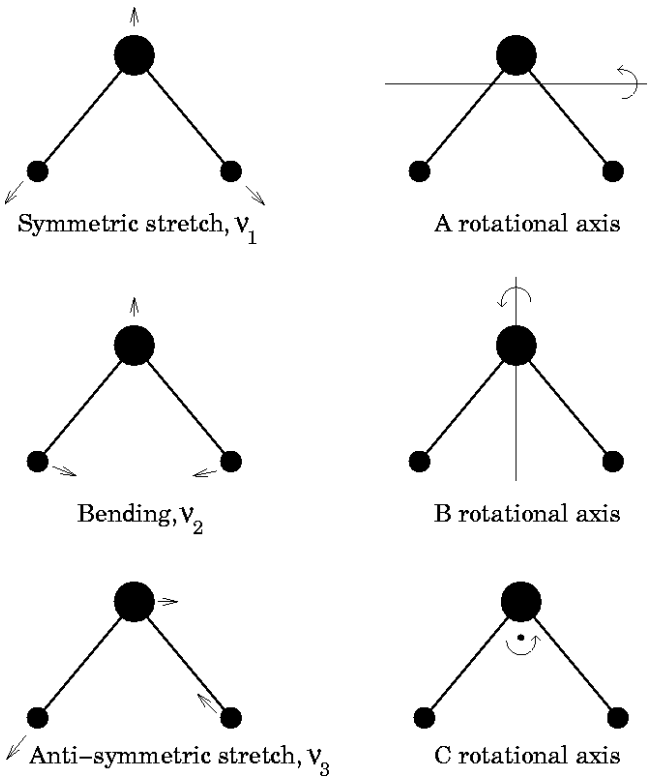

Figure 1.2: Vibrational and rotational motions of the water molecule (Tennyson & Polyansky 1998). Note the displacement of the oxygen atom as the center of mass of the entire molecule changes for the different normal modes of vibration.

vibrations and rotations, we mean that the molecule is promoted to a state of higher energy. In this, electrons are redistributed and the vibrational amplitude and rotational frequency increased. Fig. 1.1 plots the energy level diagram of a molecule, in which electronic, vibrational and rotational transitions are denoted.

To understand an observed spectrum, one first needs to know what the structure of the observed atom/molecule is. Evidently, H_2O is composed of one oxygen atom and two hydrogen atoms. Each hydrogen atom is covalently bonded to the oxygen via a shared pair of electrons. Oxygen also has two unshared pairs of electrons. Thus, in total, four pairs of electrons surround the oxygen atom; two pairs involved in covalent bonds with hydrogen, and two unshared pairs on the opposite side of the oxygen atom. Due to the unshared pairs of electrons, water has a partial negative charge near

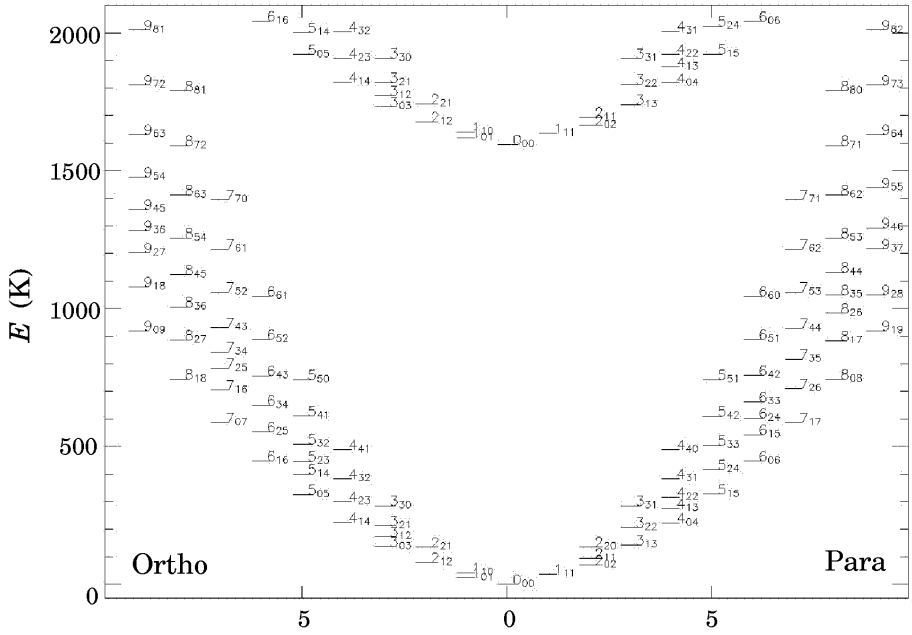

Figure 1.3: Diagram of the rotational levels of the ground and first-excited vibrational state of ortho- and para-H_2O up to an energy of 2000 K (Tielens 2005).

the oxygen atom, and partial positive charges near the hydrogen atoms. Therefore, water is referred to as a *polar* molecule, meaning that there is an uneven distribution of electron density. Because each of the hydrogen atoms has a nuclear spin 1/2, they can combine to a singlet ($S = 0$) or a triplet ($S = 1$). As such, H_2O is split into para-H_2O (p-H_2O) and ortho-H_2O (o-H_2O), respectively, between which transitions are highly forbidden ($\Delta S \neq 0$). Therefore, o- and p-H_2O can be treated as separate species since their levels are not connected by radiative transitions.

Electronic spectroscopy is important to understand a spectrum. However, in this thesis the water molecule will be mainly excited by collisions in the temperature regime $10\,\mathrm{K} \lesssim T \lesssim 1000\,\mathrm{K}$. Therefore, we will solely focus on the different vibrational and rotational states of the water molecule.

In general, a non-linear molecule with N atoms will have $3N-6$ normal modes of vibration. The vibrational modes for H_2O are (i) symmetric stretch, (ii) bending and (iii) asymmetric stretch designated with the vibrational quantum numbers ν_1, ν_2 and ν_3, respectively. The vibrational energy

Table 1.1: Characteristics of the lowest 20 ground-vibrational rotational levels for the water molecule.

Level	Energy (cm^{-1})*	J	K_a	K_c	Level	Energy (cm^{-1})	J	K_a	K_c
Para levels									
1	0.00000	0	0	0	11	315.779	4	2	2
2	37.1371	1	1	1	12	326.625	5	1	5
3	70.0907	2	0	2	13	383.842	4	3	1
4	95.1757	2	1	1	14	416.208	5	2	4
5	136.164	2	2	0	15	446.697	6	0	6
6	142.278	3	1	3	16	488.134	4	4	0
7	206.301	3	2	2	17	503.968	5	3	3
8	222.052	4	0	4	18	542.907	6	1	5
9	275.497	4	1	3	19	586.480	7	1	7
10	285.220	3	3	1	20	602.774	6	2	4
Ortho levels									
1	23.7943	1	0	1	11	325.348	5	0	5
2	42.3717	1	1	0	12	382.517	4	3	2
3	79.4963	2	1	2	13	399.458	5	1	4
4	134.901	2	2	1	14	446.510	5	2	3
5	136.761	3	0	3	15	447.252	6	1	6
6	173.365	3	1	2	16	488.108	4	4	1
7	212.156	3	2	1	17	508.812	5	3	2
8	224.838	4	1	4	18	552.911	6	2	5
9	285.419	3	3	0	19	586.244	7	0	7
10	300.362	4	2	3	20	610.341	5	4	1

* To convert to Kelvin (K), multiply by $c \times h/k$, with c the speed of light, h Planck's constant, and k the Boltzmann constant.

states correspond to particular internuclear distances; when the distance becomes so large that the atoms are no longer bound together, dissociation has occured. Besides this, three rotational, mutually perpendicular, axes passing through the center of mass permit the molecule to rotate, resulting in discrete rotational energy levels. Thanks to the peculiar geometry (triatomic asymmetric top), water can be found in many different rotational/vibrational states. The different vibrational and rotational states of the molecule are shown in Fig. 1.2.

A full description of the treatment to compute the energy level structure of water is beyond the scope of this chapter. However, it is necessary to know that the rotational levels are labeled using the standard asymmetric top notation $J_{K_aK_c}$, where J is the main rotational quantum number, and K_a and K_c its projections on the two molecular axes A and C, respectively, with $K_a + K_c = J$ or $J+1$. The molecular axes correspond to the symmetry

axis the molecule would have had in the limit that it became, respectively, either a symmetric prolate or oblate rotor, between which water is intermediate. To distinguish between prolate and oblate (a)symmetric molecules, one makes use of the moment of inertia I of the molecule. Molecules for which $I_A < I_B = I_C$ are called prolate symmetric tops, whereas oblate symmetric tops are molecules for which $I_A = I_B < I_C$. For water holds that I_A (= 0.6115 amu Å^2, amu = atomic mass unit) $\lesssim I_B$ (= 1.148 amu Å^2) $< I_C$ (= 1.760 amu Å^2), making it an asymmetric near-oblate top.

The water energy levels divide into two groups with distinct properties (see Fig. 1.3). The first group includes the lowest level of each J-state, the second one all the others. Transitions among members of the first group have larger cross sections. Because of the large collisional rates, the corresponding levels thermalize easily and carry the bulk of the population. For this reason, the levels of the first group are named the *backbone* levels. The main mode for population of off-backbone levels is a cascade from neigbouring backbone levels; all other pumping processes have much lower rates. As a result, level populations decrease with distance from the backbone ladder and each backbone level generates a trail of inverted transitions (*masers*). Large Einstein-A coefficients between the levels lead to high critical densities, of the order of 10^8 cm^{-3} or higher. The critical density n_{cr} is defined as the ratio of the Einstein-A coefficient over the collisional de-excitation rate coefficient, and is the density at which collisions dominate the de-excitation process. As such, the level populations are in local thermodynamic equilibrium (LTE) for $n > n_{cr}$ and are then given by the Boltzmann expression at the kinetic temperature of the gas, i.e.,

$$\frac{n_i}{n_j} = \frac{g_i}{g_j} \frac{\exp[-E_{ij}/kT]}{1 + \frac{n_{cr}}{n}}, \tag{1.7}$$

with n_i and n_j the population density of the ith and jth level, g_i and g_j the statistical weights of the upper and lower level, and E_{ij} the energy difference between the two levels. These high densities are obviously found in star-forming regions. However, in general the molecule is not in LTE, making radiative transfer programs valuable and necessary tools for the modeling of the molecule. The energy levels for the lowest rotational levels up to an energy of 600 cm^{-1} are listed in Table 1.1.

Due to the complex structure and spectroscopic properties of the H_2O molecule as described above, large variations in optical depths of the lines are found. Moreover, all these transitions interact with each other in that photons from, e.g., an optically thick transition will be absorbed and re-emitted in the same or other lines further into the cloud. This makes radiative transfer of water different from the majority of other molecules. As a consequence, the transfer problem is far from easy and needs to be treated as such.

1.4 Observational studies of water

A number of reasons make the water molecule important to observe. First of all, water is present in multiple sites throughout the Universe. As an example, let us take the water trail in regions of star formation. Water ice is present in cold (10 – 20 K), dense ($n > 10^3$ cm^{-3}) clouds. As these dense clouds are still extremely tenuous, water ice predominantly forms on grains, rather than through direct condensation. The loss of magnetic support is thought to initiate the collapse toward the formation of a protostar as these clouds become denser and, depending on the clumps' angular momentum, a protoplanetary disk. This collapse leads to elevated temperatures towards the center. As a result, many species, e.g., H_2O, sublimate and turn up in the gas-phase. This process provides a wealth of information on condensed species in the colder environments. After all the gas is removed from the collapsing envelope, the disk consists of solids ranging from dust, comets to giant planets. Many of the comets in their turn collide with existing planets, providing them with organic compounds and water. Second, it has become clear from laboratory studies that water plays a key role in the hot ($T \gtrsim 230$ K) gas-phase chemistry, e.g., in star-forming regions and protostellar disks. As a consequence, its role in the oxygen-chemistry is unquestioned, since in many circumstances it is, next to CO, the most abundant oxygen-bearing molecule, hence influencing the overall chemical composition of the gas. Third, as can be seen from Fig. 1.3, H_2O can be excited over a broad range of temperatures; from ~ 10 K up to ~ 2000 K. This makes H_2O a valuable tool to retrieve kinematical information in various astrophysical environments through multiple transition observations. Fourth, the role of water as an important coolant cannot be underestimated. Over a wide range of interstellar conditions the equilibrium gas temperature within molecular clouds is determined by the balance between heating processes and radiative cooling (e.g., Goldsmith & Langer 1978; Black 1987). Radiative cooling of dense molecular gas is of crucial importance to the star-formation process, because dense molecular cloud cores can only undergo gravitational collapse to form stars simply and solely as gravitational potential energy can be radiated away. Theoretical studies show that CO, H_2, and H_2O are the dominant coolants of molecular gas in the interstellar medium (Neufeld, Lepp & Melnick 1995). It is found that at low temperatures ($T \sim 10$ K) and low densities ($n_{H_2} \sim 10^{3-6}$ cm^{-3}) CO contributes most to the cooling. At these temperatures H_2 is ineffective as a coolant because it possesses no low-lying energy states. However, at high temperatures ($T \sim 100$ K) and low densities, H_2 is the dominant coolant because of its large abundance. This situation changes at high densities and high temperatures as H_2O cooling exceeds both CO and H_2 cooling because of its increased abundance (hot gas-phase chemistry) and the large dipole moment of the water molecule. Note that H_2O can also become a heating agent, if

pumped by IR radiation and then collisionaly de-excited.

Despite the presence of water in our atmosphere which hampers ground-based observations, H_2O was the third interstellar molecule discovered at radio wavelengths, after the HI radio emission line at 21 cm – the wavelength of the spin-flip transition between the ground-state hyperfine levels of atomic hydrogen – and the discovery of 18 cm radio radiation from the ground-state of OH (Weinreb et al. 1963). Cheung et al. (1969) detected the 22 GHz line corresponding to the 6_{16}-5_{23} transition of o-H_2O toward a number of star-forming regions. The emission was rather strong, with antenna temperatures as high as 60 K, even though the transition levels lie more than 600 K above ground. This requires substantial excitation rates of the 6_{16} state. Maser emission was suspected, and confirmed by the observations of Knowles et al. (1969). However, in order to observe non-masing transitions of the molecule in the infrared region of the spectrum, satellites are needed to avoid atmospheric lines. The *Infrared Space Observatory* (ISO) and the *Submillimeter Wave Astronomy Satellite* (SWAS) provided the first opportunities for sensitive searches of emission and absorption characteristics of H_2O and its isotope $H_2^{18}O$, followed by Odin. Among some of the highlights of these missions are the detection of gas-phase H_2O lines in warm star-forming regions, including the ν_2 ro-vibrational lines around 6 μm in absorption (van Dishoeck & Helmich 1996; Dartois et al. 1998) and emission (González-Alfonso et al. 1998), the detection of strong H_2O emission and absorption lines towards Orion (Harwit et al. 1998; Cernicharo et al. 1999), the detection of strong far-infrared H_2O lines toward molecular outflows (e.g., Giannini et al. 2001), observations of the water production in several comets at high spectral resolution (Lecacheux et al. 2003), the observation of H_2O emission and absorption in the direction of the Galactic Center (Sgr A) (Moneti et al. 2001; Sandqvist et al. 2003), the study of dense and diffuse interstellar gas clouds (Melnick & Bergin 2005), LWS/SWS studies of H_2O in circumstellar envelopes (Barlow 1999), planetary atmospheres (Coustenis et al. 1998), comets (Neufeld et al. 2000), and water around carbon-rich stars like IRC+10216 (Ford & Neufeld 2001).

These observations have revealed large variations in the H_2O abundances, from 10^{-8} in cold clouds to 10^{-4} in warm gas and shocks. The high water abundances in warm regions can be explained by a combination of two processes. The first being ice evaporation in regions where $T_{\rm dust} \gtrsim 100$ K, the second through high-temperature gas-phase chemistry at $T_{\rm gas} > 230$ K (Section 1.2). Nevertheless, the low abundances of H_2O (and O_2) found by SWAS on large scales in quiescent clouds are inconsistent with standard pure gas-phase chemistry models. One way to explain this deficiency is to include gas-grain chemistry and freeze-out onto interstellar grains (Bergin et al. 2000). In this, oxygen and carbon collide with grains and are transformed into solid H_2O and CH_4, followed by evaporation of the weakly bound CH_4 into the gas-phase, in comparison to the strongly

bound H_2O. As a result, the low gas-phase oxygen abundance naturally explains little O_2 and H_2O in the gas-phase. An alternative explanation has been proposed by Spaans & van Dishoeck (2001) in which the inhomogeneous nature of molecular clouds, as known from [CI] and [CII] fine-structure line observations, lowers the column densities of H_2O and O_2 by more than an order of magnitude at the same visual extinction A_V, as compared to homogeneous models, due to enhanced photo-dissociation. Note that these models were aimed at the larger scale, lower density molecular cloud regime where freeze-out is not important.

The future of the study of the infrared part of the spectrum ($1\,\mu$m – $1000\,\mu$m) – a wavelength regime that allows star-forming regions to be probed in an unprecedented way – and more specifically the study of the distribution and behaviour of water, is secured with the *Herschel Space Observatory* and the *Atacama Large Millimeter / submillimeter Array* (ALMA).

1.5 The thesis

The aim of the thesis is to achieve a better understanding of the excitation characteristics of H_2O. This is important in the interpretation of already existing observations. Besides this, future missions demand the need for sophisticated tools, since these will have better spectral and angular resolution. To this end, a fully three-dimensional spherical multi-zone escape probability method – β3D – has been developed that includes the effects of dust pumping on the level populations, and can treat (if applicable) inhomogeneity and systematic velocity fields. Chapter 2 is used to describe and test this method against existing radiative transfer codes. It is found that β3D produces level populations that agree well with the outcome of Monte Carlo (MC) and Accelerated Lambda Iterations (ALI) codes within, depending on the adopted problem, $\sim 5\%$. In Chapter 3 we apply this method to the star-forming region S140. This object consists of a photon dominated region (PDR) and an extended molecular cloud (EMC). The water emission is calculated for both regions since the excitation conditions differ between them. This is compared with the emissivity characteristics of an embedded source, known to be present in the PDR. Also, line profiles are presented for the embedded source and the PDR. It is found that due to the intrinsic different physical structure of the two objects the ground-state transitions are the strongest emitters in the PDR, whereas in the embedded source high-lying transitions produce the bulk of the emission. Chapter 4 explores the information content of the ground-state transition of o-H_2O at 557 GHz in dense molecular clouds, i.e., can this transition be used to trace a clouds' volume? We show that the intensity scales with column density in the optically thin regime. However, when the line increases in optical depth, it reaches a regime where it is even not effectively optically thin. At this

point, information is lost, and the intensity of the ground-state line does not scale linear with the column density. Hence, one can underestimate the water column density by a factor of a few when relying on single transition observations. Chapter 5 is devoted to AFGL 2591, a prototype of a high-mass star-forming region. Intensities and line profiles are presented for the different transitions of o- and p-H_2O in order to extract line diagnostics in the aformentioned region. We find that low-lying transitions are primarily sensitive to the excitation conditions of the outer regions. In contrary, high-lying transitions can be used to probe the inner parts of the system. In Chapter 6 focus is on the water emission characteristics in proto-stellar disks in the light of future SOFIA observations. The snow-line in proto-planetary disks is very important since it is thought to play a crucial role in the proces of planet formation. We find that intensities and line profiles of fluorescent water transitions around 6 μm depend strongly on the adopted dust properties and vary with freeze-out temperatures (110 –170 K). Hence, fluorescent transitions around 6 μm are sensitive probes of the snow-line transition, and can be used in the future, together with 2.3 μm fluorescent lines, to probe its location.

References

Barlow, M. J. 1999, in IAU Symp. 191: Asymptotic Giant Branch Stars, ed. T. Le Bertre, A. Lebre, & C. Waelkens, 353

Bergin, E. A., Langer, W. D., & Goldsmith, P. F. 1995, ApJ, 441, 222

Bergin, E. A., Melnick, G. J., Stauffer, J. R., et al. 2000, ApJ, 539, L129

Black, J. H. 1987, in ASSL Vol. 134, Interstellar Processes (Dordrecht: Reidel), 731

Cernicharo, J., Pardo, J. R., & González-Alfonso, E. 1999, ApJ, 520, L131

Charnley, S. B. 1997, ApJ, 481, 396

Cheung, A. C., Rank, D. M., Townes, C. H., Thornton, D. D., & Welch, W. J. 1969, Nature 221, 626

Coustenis, A., Salama, A., Lellouch, E., et al. 1998, A&A, 336, 85

Dartois, E., d'Hendecourt,L., Boulanger, F., Jourdain de Muizon, M., Breitfellner, M., Puget, J-L, & Habing, H. J. 1998, A&A, 331, 651

Doty, S. D., van Dishoeck, E. F., van der Tak, F. F. S., & Boonman, A. M. S. 2002, A&A, 389, 446

Ford, K. E. S., & Neufeld, D. A. 2001, ApJ, 557, L113

Giannini, T., Nisini, B., & Lorenzetti, D. 2001, ApJ, 555, 40

Goldsmith, P. F., & Langer, W. D. 1978, ApJ, 222, 881

González-Alfonso, E., Cernicharo, J., van Dishoeck, E. F., Wright, C. M., & Heras, A. 1998, ApJ, 502, L169

Harwit, M., Neufeld, D. A., Melnick, G. J., & Kaufman, M. J. 1998, ApJ, 497, L105

Knowles, S. H., Mayer, C. H., Cheung, A. C., Rank, D. M., & Townes, C. H. 1969, Science 163, 1005

Lee, H.-H., Bettens, R. P. A., & Herbst, E. 1996, A&AS, 119, 111

Lecacheux, A., Biver, N., Crovisier, J., et al. 2003, A&A, 402, L55

Le Teuff, Y. H., Millar, T. J., & Markwick, A. J. 2000, A&AS, 146, 157

Meijerink, R., & Spaans, M. 2005, A&A, 436, 397

Melnick, G. J., & Bergin, E. A. 2005, AdSpR, 36, 1027

Moneti, A., Cernicharo, J., & Pardo, J. R. 2001, ApJ, 549, L203
Neufeld, D. A., Lepp, S., & Melnick, G. J. 1995, ApJS, 100, 132
Neufeld, D. A., Stauffer, J. R., Bergin, E. A., et al. 2000, ApJ, 539, 151
Sandqvist, A., Bergman, P., Black, J. H., et al. 2003, A&A, 402, L63
Spaans, M., & van Dishoeck, E. F. 2001, ApJ, 548, L217
Stäuber, P., Jørgensen, J. K., van Dishoeck, E. F., Doty, S. D., & Benz, A. O. 2006, A&A, 453, 555
Tennyson, J., & Polyansky, O. L. 1998, Contemporary Physics, volume 39, number 4, pages 183-294
Tielens, A. G. G. M. 2005, The Physics and Chemistry of the Interstellar Medium (The Physics and Chemistry of the Interstellar medium, by A. G. G. M. Tielens, ISBN 0521826349 Cambridge, UK: Cambridge University press, 2005.)
van Dishoeck, E. F., & Helmich, F. P. 1996, A&A, 315, L177
Weinreb, S., Barrett, A. H., Meeks, M. L., & Henry, J. C. 1963, Nature 200, 829
Willacy, K. 2004, ApJ, 600, L87